Skeletal Radiol (1993) 22:37–41

Skeletal Radiology

Soft tissue edema in osteoid osteoma

Jean-Christophe Biebuyck, M.D.[1], Lee D. Katz, M.D.[1,2,3], and Thomas McCauley, M.D.[1]

Departments of [1] Diagnostic Radiology, [2] Internal Medicine, and [3] Orthopaedics and Rehabilitation, Yale University School of Medicine, New Haven, Connecticut, USA

Abstract. Four cases of osteoid osteomas are presented. An uncharacteristic magnetic resonance finding of soft tissue edema is reported. This observation should not be misinterpreted as indicating a more aggressive pathologic process and, thereby, exclude osteoid osteoma from the differential.

Key words: Osteoid osteoma – Magnetic resonance imaging – Osteomyclitis – Bone tumors

Jaffe originally described osteoid osteomas in 1935 [17]. Since then, our understanding of these lesions has grown immensely. Conventional radiographs, plain film tomography, bones scans, and computerized tomography have served as the classic imaging approach in evaluating these lesions' clinical and radiographic features. More recently, magnetic resonance imaging (MRI) has offered a new modality with which to study osteoid osteomas. In this paper, four cases of osteoid osteoma are presented and an uncharacteristic MRI finding is reported; soft tissue edema. This finding influenced the preoperative radiologic diagnosis of these cases, and may therefore act as a pitfall in attaining the correct diagnosis.

Case reports

Case 1

The patient is a 5-year-old boy without significant past medial history. He presented to his pediatrician with a 2.5-month history of right groin and right medial thigh pain. The pain woke the patient from sleep and was promptly relieved by ibuprofen. Physical examination revealed decreased muscle bulk in the right thigh. There were no signs of inflammation. Erythrocyte sedimentation rate (ESR) was 23. Other laboratory findings were normal. Bilateral hip films from an outside hospital were reported to be normal. The patient was referred to this institution for right hip radiographs (Fig. 1A) and a bone scan (Fig. 1B). The radiographs revealed periosteal thickening in the right femoral neck adjacent to the lesser trochanter. The bone scan revealed diffuse increased activity in the right hip with a curvilinear focus in the region of the lesser trochanter. These findings were felt to be consistent with osteomyelitis or an osteoid osteoma and MRI was recommended for further evaluation. MRI examination of the hips demonstrated a high-signal lesion in the right femoral neck which corresponded to the findings on the plain film radiographs. There was diffuse edema involving the femoral neck and extending down into the shaft of the femur (Fig. 1C). A joint effusion was present. In addition, there was edema of the adductor muscles adjacent to this lesion. These findings were again considered to be secondary to a focus of osteomyelitis (Brodie's abscess) or an osteoid osteoma. The pathologic specimen demonstrated an osteoid osteoma.

Correspondence to: Lee D. Katz, M.D., Yale University School of Medicine, Department of Diagnostic Radiology, 333 Cedar Street, New Haven, CT 06510, USA

Case 2

The patient is a 6-year-old boy without significant past medical history. He presented to his pediatrician with a 4-month history of left knee pain localized to the popliteal fossa. Physical examination was normal. Laboratory examination was unremarkable. A left hip film showed an eccentric posteriorly located focal lytic lesion in the distal femur (Fig. 2A, B). This was surrounded by a dense cortical reaction. A bone scan revealed diffuse uptake in the distal femur (Fig. 2C). An MRI was obtained for further evaluation. This revealed a 1-cm round lesion which had an intermediate signal on the first echo and a high signal on the second echo (Fig. 2D). There was evidence of soft tissue edema. The preoperative diagnosis was osteomyelitis. A histologic specimen obtained at surgery revealed an osteoid osteoma.

Case 3

The patient is a 13-year-old boy without significant past medical history. He had pain in his left third finger and progressive enlargement of the distal phalanx for 1 year. Physical examination revealed an enlarged, tender distal phalanx of the left third finger. Laboratory examination was unremarkable. Plain films of the hand showed soft tissue swelling, and a subungual lesion of the third finger's distal phalanx. A real-time color flow duplex Doppler evaluation, before an excisional biopsy, showed bidirectional flow in

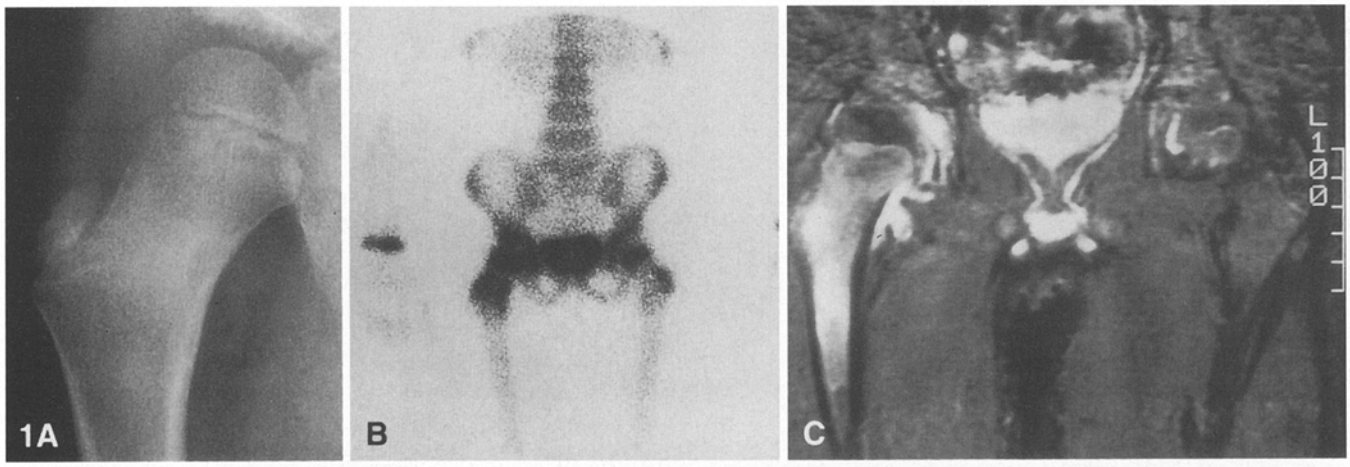

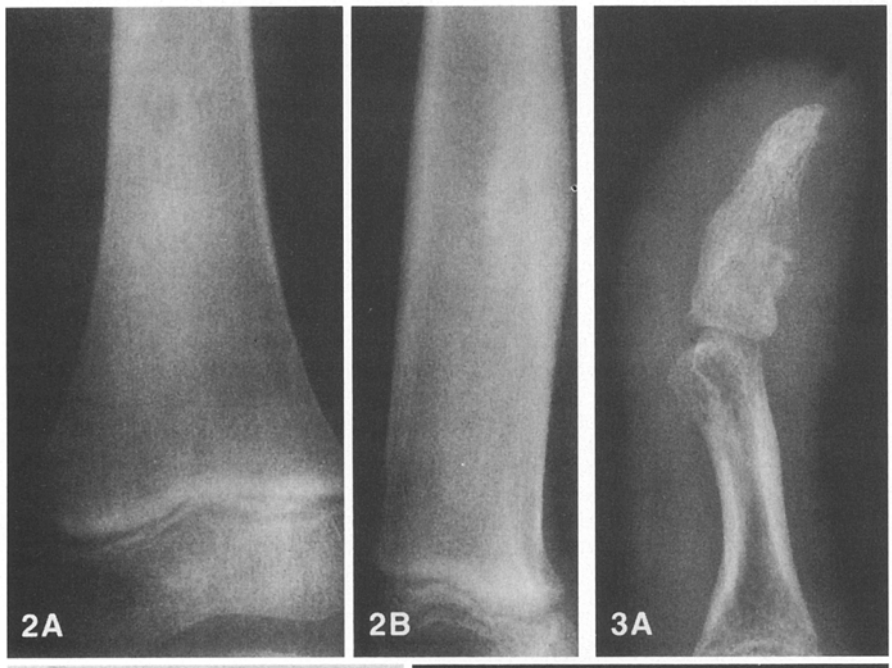

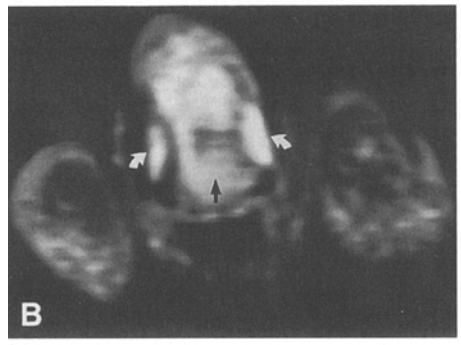

Fig. 1. A Anteroposterior radiograph of the right femur demonstrates a sclerotic zone adjacent to the lesser trochanter with a lucent central zone. **B** ^{99m}Technetium-MDP bone scan shows uptake in the right femoral neck and lesser trochanter. **C** Inversion recovery MRI (TR 2000/TE 40/TI 140) demonstrates edema within the soft tissues adjacent to the lesion, a hip effusion and edema throughout the proximal femur extending into the diaphysis

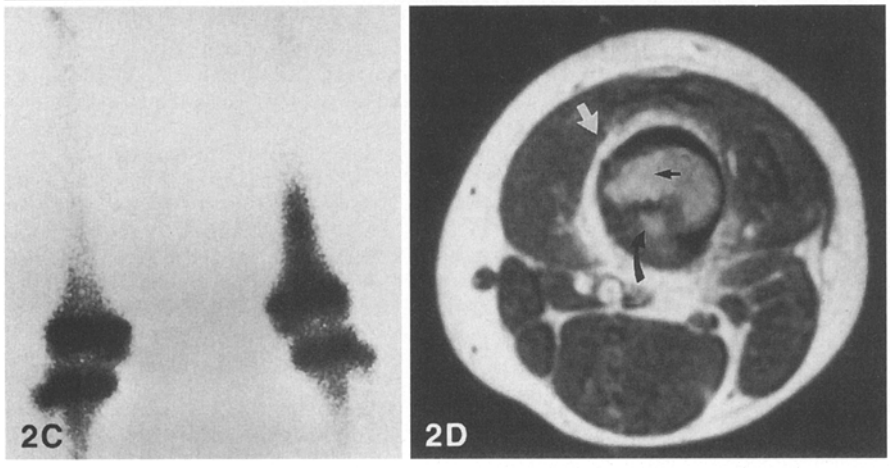

Fig. 2. A, B Anteroposterior and lateral radiographs of the distal left femur demonstrate an eccentric lesion with sclerosis and focal periosteal reaction. **C** ^{99m}Technetium-MDP bone scan demonstrates diffuse uptake involving the distal left femur. **D** Axial MRI (TR 2000/TE 80) demonstrates edema surrounding the femur (*white arrow*), edema within the bone marrow (*black arrow*) and central nidus within the sclerotic bone which has high signal (*curved black arrow*)

Fig. 3. A Lateral radiograph of the terminal phalanx demonstrates an eccentric lesion which has expanded the bone and has a calcified matrix. In addition, there is soft tissue swelling. **B** Coronal inversion recovery MRI (TR 1400/TE 43/TI 140) demonstrates edema within the marrow of the terminal phalanx (*solid arrow*) and soft tissue edema (*curved arrows*)

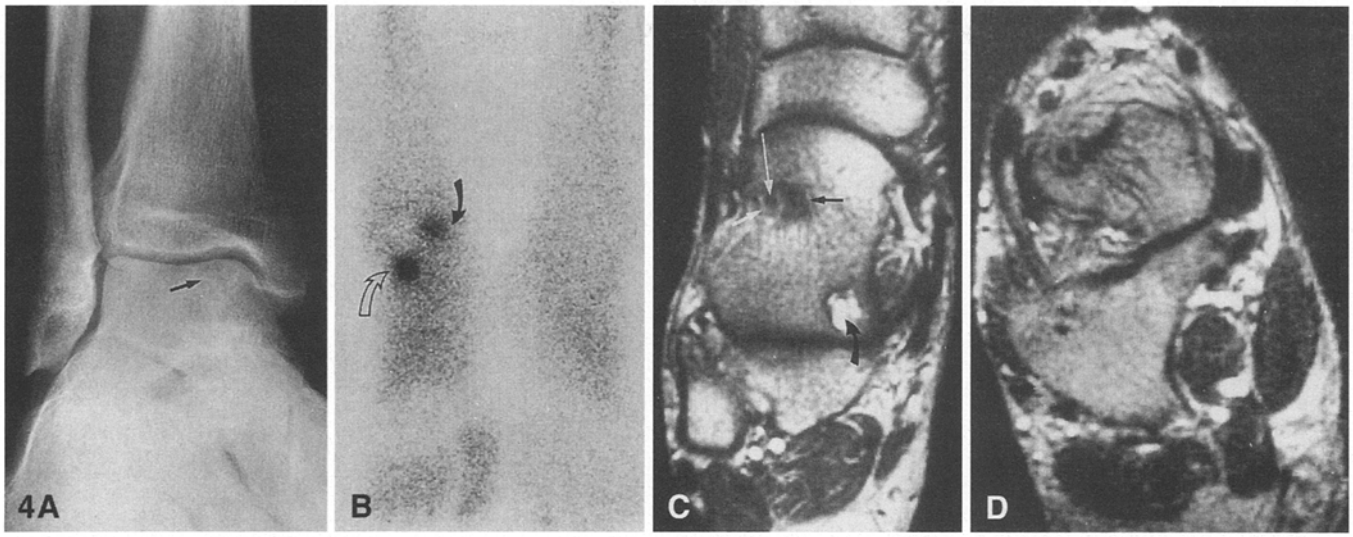

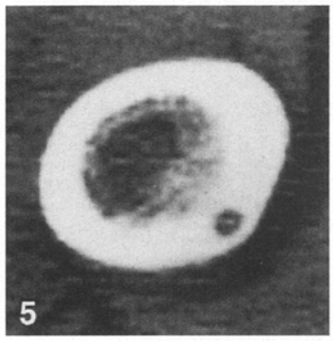

Fig. 4. **A** An oblique view of the ankle demonstrates a lucent lesion in the superior medial portion of the talus (*arrow*). **B** ^{99m}Technetium-MDP bone scan demonstrates two lesions. An area of increased activity seen in the superior medial portion of the talus (*curved arrow*) is consistent with the plain film finding. A second lesion (*curved open arrow*) is seen in the distal talus. **C, D** Axial T2-weighted MRI scans (TR 1500/TE 80) demonstrate an area of central signal void (*long white arrow*), surrounded by an area of higher signal (*short white arrow*), surrounded again by signal void (*short black arrow*). This is consistent with osteoid osteoma. The area of OCD is noted (*curved black arrow*). Diffuse soft tissue edema is seen as surrounding the area of the lesion

Fig. 5. CT scan through the midshaft of the femur demonstrates a lucent zone within the cortex with a central calcification consistent with a diagnosis of osteoid osteoma

multiple vessels. It was felt that this finding correlated with a glomus tumor. The initial biopsy revealed fibroadipose tissue. The patient continued to have pain and was referred to this institution. Repeat plain films showed an eccentrically located lytic lesion of the dorsal aspect of the distal phalanx with ill-defined borders and a calcified matrix (Fig. 3A). In addition, periosteal thickening and posterior expansion were noted. An MRI was obtained for further evaluation. This showed an abnormal signal within the distal phalanx which increased on T2-weighted images (Fig. 3B). In the subungual region there was an area of low signal intensity on the T2 images. This corresponded to the calcified lytic lesion on the plain film. Marked soft tissue edema was noted adjacent to this lesion. A preoperative differential diagnosis included a glomus tumor, osteomyelitis, and osteoid osteoma. A histologic specimen revealed an osteoid osteoma.

Case 4

The patient is a 31-year-old man who developed ankle pain 7 years prior to being seen at this institution. He states that the pain progressively worsened over the last 3 years. The patient had a previous diagnosis of osteochondritis dissecans (OCD) of the talus. His physical examination was remarkable for tenderness on palpation over the dorsum of the right talus. A laboratory workup was unremarkable. Plain films of the ankle showed a lucent lesion of the superior medial portion of the talus (Fig. 4A). A bone scan revealed two areas of increased uptake in the talus (Fig. 4B). One corresponded to the abnormal trabecular pattern seen on the plain film. Another area of increased uptake was seen in the distal talus. This was believed to be secondary to avascular necrosis or osteomyelitis. MRI showed a signal abnormality in the superior medial portion of the talus containing fluid consistent with the diagnosis of OCD. In addition, a second lesion was noted in the talar head (Fig. 4C, D), having concentric zones of various signals. There was an inner zone of low signal, surrounded by a zone of intermediate signal which became bright on the second echo, surrounded by a zone of low signal. Soft tissue edema was noted in conjunction with this second lesion. An operative histologic specimen of this second lesion revealed an osteoid osteoma.

Discussion

Osteoid osteomas are benign neoplasms. They are composed of a central nidus with surrounding densely sclerotic bone. Histopathologically, the nidus is composed of a branching array of incompletely ossified trabeculae [2]. These trabeculae are separated by exuberantly vascularized connective tissue. Ultrastructurally, the nidus is composed of osteoblasts [31].

Histologically, osteoid osteomas resemble osteoblastomas [27]. Osteoblastomas are uniformly larger and tend to have a different skeletal distribution [8, 16, 18]. For these reasons, Jaffe unequivocally rejected the nomenclature of "giant" osteoid osteomas to describe osteoblastomas. Instead, he divided osteoblastic tumors by size. Those less than 1 cm in size were categorized as osteoid osteomas. Those greater than 2 cm were termed osteoblastomas [19].

Osteoid osteomas are most frequently diaphyseal lesions of the tibia and femur [18]. They may extend into the metaphysis or, more rarely, present as a pure epiphyseal or intra-articular lesion [5, 6, 28]. They may present as lesions in the foot, hand, wrist, spine, or arm. Unusual locations have been described [3, 4, 9, 13, 22, 26, 30]. Males are affected three times more often than females. The lesions may present in patients at almost any age, but most typically during the second decade of life [12].

Patients with osteoid osteomas most commonly present with a history of pain. Characteristically, this pain is worse at night and relieved by salicylates and other nonsteroidal anti-inflammatory medications [23]. Both prostaglandins (PGE_2) and autonomic nerve fibers have been implicated as the causitive pain-provoking agent [21, 29].

Conventional radiographs classically demonstrate a radiolucent nidus measuring less than 1 cm in diameter surrounded by exuberant reactive sclerotic bone. The constellation of these findings is not uniformly present and may be different according to the location of the nidus [7]. The radiolucent nidus may be obscured by the adjacent reactive sclerosis. CT scanning may be required to pinpoint the nidus's exact location. Calcifications within the nidus may be more clearly seen on CT scanning and help differentiate the lesion from other pathologic processes [10, 11]. Osteoid osteomas avidly acquire radiopharmaceuticals in the vascular, blood-pool, and delayed phases of bone scintigraphy. A classic double-density sign has been observed. The central nidus accumulates the radionuclide more than the surrounding sclerotic bone. This results in an intense central scintigraphic activity with relatively decreased activity in the adjacent bone. This double-density pattern may help differentiate osteoid osteomas from osteomyelitis or a Brodie's abscess [14, 20].

Although CT is superior to MRI in detecting an osteoid osteoma [33] (Fig. 5), MRI has been useful in characterizing the intraosseous, soft tissue, and intramedullary extent of the lesion because of its increased contrast resolution. In the cases presented, the unexpected finding of soft tissue edema is one more example of potential error that may arise from attempting to diagnose a lesion based entirely on the MR appearance. When a classic history and radiographs are present, the diagnosis can easily be made. CT is then the examination of choice for confirming the diagnosis and pinpointing the exact location of the tumor for surgical resection. In children, MRI is usually performed first in order to limit radiation exposure [1, 25, 32, 34]. If the nidus is not apparent and the history not straightforward, then MRI may demonstrate the presence of soft tissue edema, which may lead to a delayed or erroneous diagnosis such as infection.

The MRI appearance of osteoid osteoma has been described. The nidus can have one of three appearances. Intermediate T1 and high T2 MR signals have been described. Although controversial, a "cystic" appearance of low T1 and high T2 signals and a "sclerotic" appearance of low T1 and T2 signals can be seen. Perinidal sclerosis typically is demonstrated by a low T1 and variable T2 signal. Increasing heterogeneity of the T2 signal corresponds with increasing tumor size and severity of symptoms [24]. Low T1 and high T2 signals within the medullary space correspond to marrow edema [15].

In conclusion, four cases of osteoid osteoma have been presented which show characteristics of soft tissue edema in addition to their typical marrow abnormalities. The finding of soft tissue edema, not previously reported with osteoid osteoma, should not be misinterpreted as indicating a more aggressive pathologic process.

References

1. Bohndorf K, Reiser M, Lochner B, et al (1986) Magnetic resonance imaging of primary tumors and tumor-like lesions of bone. Skeletal Radiol 15:511
2. Byers PD (1968) Solitary benign osteoblastic lesions of bone: osteoid osteoma and osteoblastoma. Cancer 22:43
3. Caldicott WJH (1969) Diagnosis of spinal osteoid osteoma. Radiology 92:1192
4. Carroll RE (1953) Osteoid osteoma in the hand. J Bone Joint Surg (Am) 35:888
5. Corbett JM, Wilde AH, McCormack LJ, et al (1974) Intra-articular osteoid osteoma: a diagnostic problem. Clin Orth Rel Res 98:225
6. Cronemyer RL, Kirchmer NA, DeSmet AA, et al (1981) Intra-articular osteoid-osteoma of the humerus simulating synovits of the elbow. A case report. J Bone Joint Surg (Am) 63:1172
7. Dahlin DC, Unni KK (1986) Bone tumors: general aspects and data on 8,542 cases, 4th edn. Thomas, Springfield, pp 102–118
8. Dias LDS, Frost HM (1974) Osteoid osteoma – osteoblastoma. Cancer 33:1075
9. Freiberger RH, Loitman BS, Halpern M, et al (1959) Osteoid osteomas: a report of 80 cases. Am J Roentgenol 82:194
10. Gamba JL, Martinez S, Apple J, et al (1959) Computed tomography of axial skeletal osteoid osteomas. Am J of Roentgenol 142:769
11. Ghelman B (1989) Radiology of bone tumors. Orth Clin NA 20:287
12. Gitelis S, Schajowicz F (1989) Osteoid osteoma and osteoblastoma. Orth Clin NA 20:313
13. Golding JSR (1954) The natural history of osteoid osteoma with a report of twenty cases. J Bone Joint Surg (Br) 36:218
14. Helms CA, Hattner RS, Vogler JB (1984) Osteoid osteoma: radionuclide diagnosis. Radiol 151:779
15. Helms CA, et al (1989) Tumors. Musculoskeletal magnetic resonance imaging
16. Jackson RP, Reckling RW, Mantz FA (1977) Osteoid osteoma and osteoblastoma: similar histologic lesions with different natural histories. Clin Orth 128:303
17. Jaffe HL (1935) "Osteoid osteoma": a benign osteoblastic tumor composed of osteoid and atypical bone. Arch Surg 31:709
18. Jaffe HL (1945) Osteoid osteoma of bone. Radiology 45:319
19. Jaffe HL (1956) Benign osteoblastoma. Bul Hosp Joint Dis 17:141
20. Lisbona R, Rosenthall L (1979) Role of radionuclide imaging in osteoid osteoma. Am J Roentgenol 132:77
21. Makley JT, Dunn MJ (1982) Prostaglandin synthesis by osteoid osteoma. Lancet 2:42
22. Marcove RC, Freiberger RH (1966) Osteoid osteoma of the elbow: a diagnostic problem. J Bone Joint Surg 48A:1185
23. Orlowski JP, Mercer RD (1977) Osteoid osteoma in children and young adults. Pediatrics 59:526
24. Patel M (1990) MR imaging of osteoid osteoma: new observations. RSNA Abst 356:146

25. Pettersson H, Gillespy T, Hamlin DJ, et al (1987) Primary musculoskeletal tumors: Examination with MR images compared with conventional modalities. Radiol 164:237
26. Pettine KA, Klasen RA (1986) Osteoid osteoma and osteoblastoma of the spine. J Bone Joint Surg (Am) 68:354
27. Schajowicz F, Lemos C (1970) Osteoid osteoma and osteoblastoma: closely related entities of osteoblastic derivation. Acta Orthop Scand 41:272
28. Schulman L, Dorfman HD (1970) Nerve fibers in osteoid osteoma. Bone Joint Surg 52A:1351
29. Seruzier E, Simonin JL, Ducastelle C, et al (1976) Ostéome ostéoide avec synovite. A propos de deux observations. Revue Rhum Mal Osteo 43:521
30. Sherman MS (1947) Osteoid osteoma: Review of the literature and report of thirty cases. J Bone Joint Surg (Am) 29:918
31. Steiner GC (1976) Ultrastructure of osteoid osteoma. Human Pathol 7:309
32. Stoller DW (1989) Magnetic resonance imaging in orthopedics and rheumatology. Lippincott, Philadelphia
33. Sundaram M, McGuire M (1988) Computed tomography or magnetic resonance for evaluating the solitary tumor or tumor-like lesion of bone? Skeletal Radiol 17:392
34. Zimmer WD, Berquist TH, Mcleod RA, et al (1985) Bone tumors: magnetic resonance imaging versus computed tomography. Radiology 155:709